



Enhanced catalytic activity of bio-fabricated ZnO NPs prepared by ultrasound-assisted route for the synthesis of tetraketone and benzylidenemalonitrile in hydrotropic aqueous medium

Suraj R. Attar¹ · Bipin Shinde² · Santosh B. Kamble¹

Received: 20 June 2020 / Accepted: 3 August 2020 / Published online: 15 August 2020
© Springer Nature B.V. 2020

Abstract

Mushroom-like mesoporous and hexagonal ZnO nanoparticles were synthesized from plant extract and chemical method respectively, by co-precipitation method in aqueous medium. Different morphological forms of ZnO NPs were characterized by XRD, TGA, FESEM, EDX, FTIR, UV–Vis and BET. Neem (*Azadirachta indica*) leaf extract and ultrasound irradiation have a crucial role in the formation of different morphologies of ZnO NPs. ZnO NPs synthesized from plant extract and hydro-tropes show a synergistic effect that leads to efficient synthesis of benzylidenemalonitrile and tetraketone derivatives at room temperature in water. Simple preparation of the catalyst, excellent yields, reusability of catalyst with consistent activity and ease of product isolation are the most significant advantages of this green protocol.

Electronic supplementary material The online version of this article (<https://doi.org/10.1007/s11164-020-04233-5>) contains supplementary material, which is available to authorized users.

✉ Santosh B. Kamble
santosh.san143@gmail.com

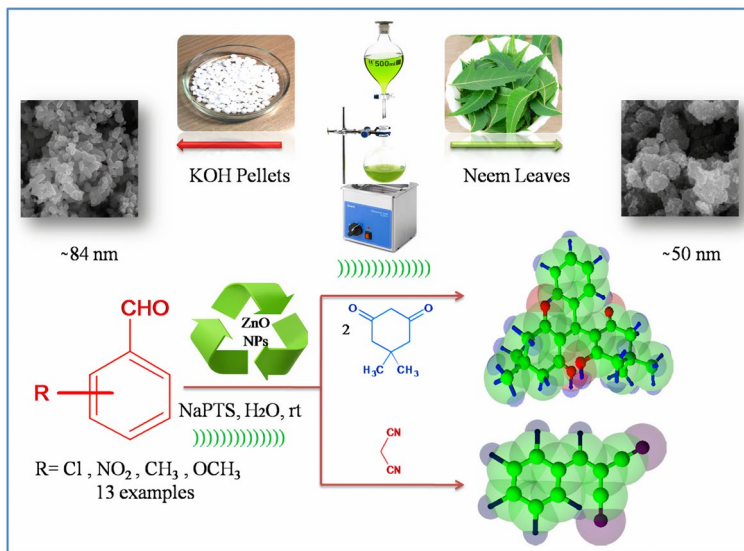
Suraj R. Attar
surajattar.chem@gmail.com

Bipin Shinde
bipinshinde448@gmail.com

¹ Department of Chemistry, Yashwantrao Chavan Institute of Science, Satara, Maharashtra, India

² Department of Chemistry, Rayat Shikshan Sanstha's Karmaveer Bhaurao Patil College Vashi, Navi Mumbai, India

Graphic abstract



Keywords ZnO nanoparticles · Heterogeneous catalysis · Hydrotrope · Knoevenagel condensation · Michael addition

Introduction

Today, the development of green processes and pollutant-free catalyst has great importance and nanotechnology offers the opportunity to create processes green from the beginning [1]. In parallel, the green synthesis of metallic and metal oxide NPs is the center of attraction for researchers as they have unusual optical, chemical, photochemical and electronic properties [2]. Among the various available nanocatalysts, ZnO nanocatalysts have attracted wide interest due to their innumerable applications and sustainable nature. ZnO NPs are used in transistors, light-emitting diodes, ultraviolet optoelectronic devices, solar cell, biosensors and photocatalysis [3]. On the other hand, they are efficiently used in many reactions such as Ugi reaction [4] and Claisen–Schmidt condensation reaction [5] because of their reactivity, selectivity, stability and reusability at elevated temperature in various solvents. Therefore, developing eco-friendly and cost-effective method for the synthesis of ZnO NPs with controlled morphology is a target for many scholars. Moreover, plant extract (PE) is applied in a wide range in green synthesis of metal oxide because it contains various biological active compounds. Indeed, a biosynthetic method is more efficient than chemical method (CM) as it is eco-friendly and cost-effective [6, 7].

In recent year, ultrasound irradiation has been employed as a promising approach for effective bio-fabricated synthesis of nanoparticles as compared to other methods and has been established as a green and effective technique [8, 9]. The neem (*Azadirachta indica*) leaf extract used in the present work is a rich source of biologically active compounds such as organic acids, quinines, flavones, aldehydes, amides, isoazadirolide and azadirachtin, which plays a vital role in the formation of zinc ions into nanostructured ZnO [10]. From the literature survey, neem is a traditional plant in India with innumerable medicinal values with a high concentration of zinc [11]. Moreover, that contains mainly reducing agents which acts as a capping as well as stabilizing agent [12]. Furthermore, as reported in the literature ultrasonication of aqueous plant extract not only gives rise to quick diffusion of solute out of the solvent but also enhances rate of formation of nanoparticles [13].

The Knoevenagel condensation reaction followed by Michael reaction of aldehydes with activated carbon-containing compounds is an essential and powerful tool in the synthesis of fine and biologically active chemicals [14]. Benzylidenemalonitrile (BMN) derivatives and tetraketone derivatives of aryl aldehyde are diverse groups of important organic intermediates which are valuable to many organic transformations. A review of the literature reveals many examples of heterogeneous catalysts for the Knoevenagel condensation reaction, such as basic MCM-41 silica [15], mesoporous titanasilicate [16], ZIF-8 [17], Ni(II)-based coordination polymers [18], Cd(II)-based coordination polymers [19], metal-organic framework (MOF)-NH₂ [20], Zn@ZIF-67 [21] and PdAlO(OH) [22]. Tetraketone derivatives have biological and therapeutic activities as antioxidants, tyrosinase inhibitor and lipoxygenase inhibitor [23]. Because of their great importance, a wide variety of synthetic methodologies have been developed for the synthesis of tetraketone, including EDDA [24], β -cyclodextrins [25], Al/MCM-41 [26], SmCl₃ [27], choline chloride [28] and PVP-stabilized Ni NPs [29]. However, many of these catalysts generally suffer from disadvantages such as unwanted side product, low reaction yields, tedious work-up procedures, harsh reaction conditions, toxic and expensive solvents or chemicals, prolonged reaction times and low reusability. Therefore, further efforts are needed toward development of greener synthetic methodologies for the synthesis of BMN and tetraketone. Water is the best choice as a solvent through the virtue of green chemistry, but the major drawback of using water as a solvent is its poor ability to solubilize organic reactants [30]. In this condition, hydrotrope is one of the phenomena to increase the aqueous solubility of poorly soluble solute. Hydrotrope not only solubilizes the organic compounds but also forms stable dispersion systems with an organic substrate, and this acts both as a catalyst and as a protector to create hydrophobic environment in water [31].

In the present study, we explored the morphological study of ZnO NPs synthesized from PE as well as CM. A facile and eco-friendly approach was adapted to produce ZnO NPs. For this purpose, an aqueous extract of neem (*Azadirachta indica*) leaves was used to produce ZnO NPs through a rapid ultrasound-assisted process, subsequently labeled as ZnO-PE. The morphology was characterized by XRD, FESEM, EDX, FTIR, TGA-DTA, UV-Vis and BET techniques and compared with ZnO NPs synthesized chemically in aqueous medium under ultrasound irradiation process, labeled as ZnO-CM. The catalytic activities of ZnO NPs were

evaluated by introducing an efficient recyclable catalyst for the synthesis of BMN and tetraketone in hydrotropic aqueous medium at room temperature, and the correlation between ZnO-PE and ZnO-CM nanoparticles was explored. All reactions were carried out by using the water solvent system at room temperature.

Experimental section

General

Neat and clean neem (*Azadirachta indica*) leaves were collected from botanical garden of Y.C.I.S. Satara, India. All chemicals were purchased from Loba and Sigma-Aldrich chemical companies and used without further purification. Double-distilled water was used as aqueous medium. Thermogravimetric analysis (TGA) was performed using Mettler Toledo, Switzerland (25–900 °C). Fourier transform infrared spectroscopy was performed by FTIR, Lambda, Australia, in the form of diluted sample (10 wt.%) pressed into KBr pellets. Powder X-ray diffraction (XRD) of ZnO was performed by Ultima IV, Rigaku Corporation, Japan, with monochromatic Cu K α radiation with wavelength $\lambda = 1.5406 \text{ \AA}$. The morphologies and structures of ZnO NPs were characterized by field emission scanning electron microscopy SIGMA HV equipped with energy-dispersive X-ray (EDX) spectroscopy. The ^1H NMR and ^{13}C NMR spectra were recorded on a Bruker Avance^{III}, Switzerland, in CDCl_3 solution. Melting points were determined using a melting/boiling point apparatus (EQ 730A-EQUIPTRONICS) and are uncorrected. Sonication was performed in a SPECTRALAB-UCB-30 ultrasonic bath with a frequency of 40 kHz and nominal power of 100 W.

Preparation of ZnO NPs from chemical method (ZnO-CM)

To 50 mL of 0.05 M solution of zinc acetate dihydrate in deionized water, 1 M KOH was added dropwise to maintain the pH at 10 for 1 hr at 60 °C under sonication. Sonication was carried out for another 1 hr until white precipitate formed which indicates the synthesis of ZnO nanostructures. Then, solution was centrifuged, mother liquor was removed, precipitate was washed five times with deionized water, and then, precipitate was dried in air. Calcination was carried out at 300 °C for 6 h.

Preparation of neem plant extract

Fresh leaves of neem (*Azadirachta indica*) without any infestation were collected and washed with double-distilled water to remove dust particles. The leaves were allowed to dry at room temperature and then crushed by grinding mill into fine powder. Twenty-five grams of neem leaves powder was soaked in 100 mL of double-distilled water and allowed to boil under ultrasonic irradiation at 60 °C for 30 min. Solution was cooled and then filtered with Whatman No. 42 filter paper. Finally, obtained greenish-yellow aqueous extract (neem extract) was stored in a refrigerator for a further subsequent application in the synthesis of ZnO-PE NPs.

Synthesis of ZnO NPs from plant extract (ZnO-PE)

To 50 mL of 0.05 M solution of zinc acetate dihydrate in deionized water, 25 mL of neem extract was added dropwise for 1 h at 60 °C under sonication. The pH of the mixture was then maintained at 10 by adding 1 M KOH dropwise for 1 hr at 60 °C under sonication. Sonication was carried out for another 1 hr until pale white precipitate formed which indicates the synthesis of ZnO nanostructures. Then, solution was centrifuged, mother liquor was removed, precipitate was washed five times with deionized water, and then, precipitate was dried in air. Calcination was carried out at 200 °C for 2 h.

Synthesis of benzylidenemalonitrile (BMN)

A mixture of 1 mmol of aldehyde, 1 mmol of active methylene compound, 10 mol% of ZnO NPs and 20% of NaPTS in 5 mL of water was stirred at room temperature. After completion of reaction (indicated by TLC), product was obtained by dissolving in ethyl acetate/ethanol. (NPs were separated by centrifugation.) The product was recrystallized by ethanol and characterized by IR, NMR and ^{13}C .

Synthesis of tetraketone

A mixture of 1 mmol of aldehyde, 2 mmol of active methylene compound, 10 mol% of ZnO NPs and 20% of NaPTS in 5 mL of water was stirred at room temperature. After completion of reaction (indicated by TLC), product was obtained by dissolving in ethyl acetate/ethanol. (NPs were separated by centrifugation.) The product was recrystallized by ethanol and characterized by IR, NMR and ^{13}C .

Results and discussion

The ZnO nanoparticles were prepared by two different methods, namely ‘plant extract co-precipitation method’ and ‘chemical co-precipitation method.’ A wide diversity of metabolism present in neem (*Azadirachta indica*) leaf extract possesses antioxidant or reducing properties out of which organic acid, flavones, quinines, isoazadirolide and azadirachtin are water soluble [10]. These biologically active compounds diffuse easily under ultrasonication and immediately reduce zinc ions into ZnO NPs [13]. The plausible mechanism is shown in Fig. 1. The carbonyl and phenolic compound of plant extract acts as a reducing as well as capping agent [10].

XRD Analysis

The phase purity and crystallinity of the plant extract and chemical method synthesized ZnO NPs were investigated using X-ray diffraction. The XRD patterns of the obtained ZnO NPs are shown in Fig. 2b, c. Figure 2a shows the XRD pattern

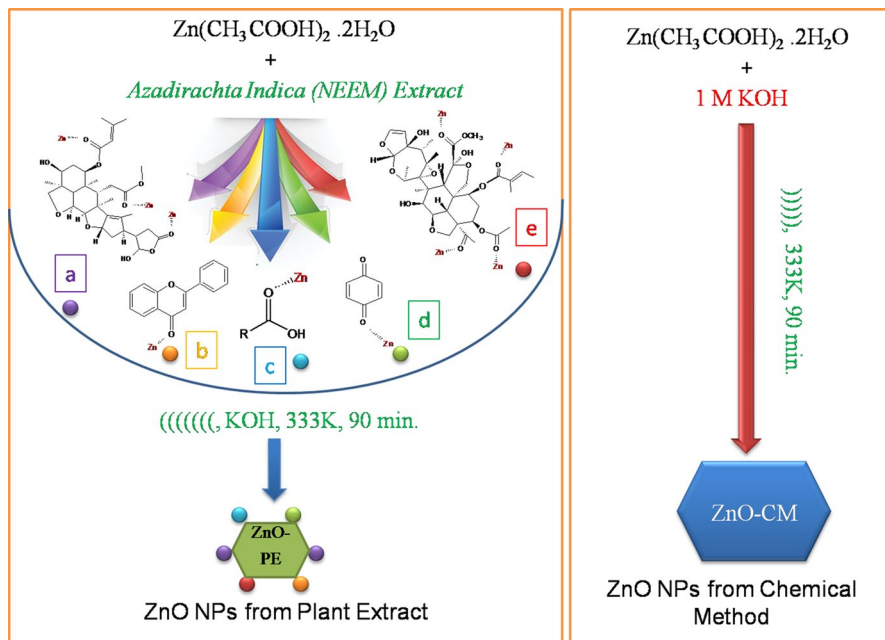


Fig.1 Plausible mechanism for the synthesis of ZnO NPs from plant extract as well as from chemical method. (a) Isoazadirolide. (b) Flavones. (c) Organic acids. (d) Quinone. (e) Azadirachtin

of ZnO synthesized from plant extract before calcination, which confirms the necessity of higher calcination temperature for the growth of crystals [32]. XRD patterns (Fig. 2b, c) indicate that both ZnO samples have a hexagonal crystal structure. The XRD pattern of the ZnO-PE NPs shows 2θ values at 31.87° , 34.46° , 36.31° , 47.63° , 56.67° , 63.12° , 66.50° , 68.06° , 69.20° , 72.58° and 77.09° and that of ZnO-CM NPs shows 2θ values at 31.94° , 34.57° , 36.43° , 47.73° , 56.76° , 63.03° , 66.54° , 68.12° , 69.23° , 72.69° and 77.17° , which correspond to (100), (002), (101), (102), (110), (103), (200), (112), (201), (004) and (202) planes of hexagonal ZnO NPs, which are consistent with standard JCPDS reported values (Table 1). No additional peaks from other phase were observed. The position of the different lines and their relative intensity matches with the standard JCPDS reported (JCPDS 36-1451) values. The XRD lines of the ZnO prepared with chemical method are relatively sharp, whereas those of ZnO prepared with plant extract are relatively broader. This broadening indicates that those materials have smaller crystallite sizes; meanwhile, peak intensities and narrow widths of XRD peaks are clear evidence of good crystallinity [33]. The average crystallite size (D) was calculated by using Debye–Scherrer formula $D = [0.9\lambda/\beta \cos\theta]$, where X-ray wavelength (λ) = 1.5406 \AA and β is the corresponding full-width at half-maximum (FWHM) values of characteristics peaks; accordingly, the average crystallite size of ZnO NPs synthesized from plant extract is about 42 nm, while that of ZnO NPs synthesized by chemical method is about 73 nm. The calculated crystallite sizes support the XRD line broadening data shown in Fig. 2. The result

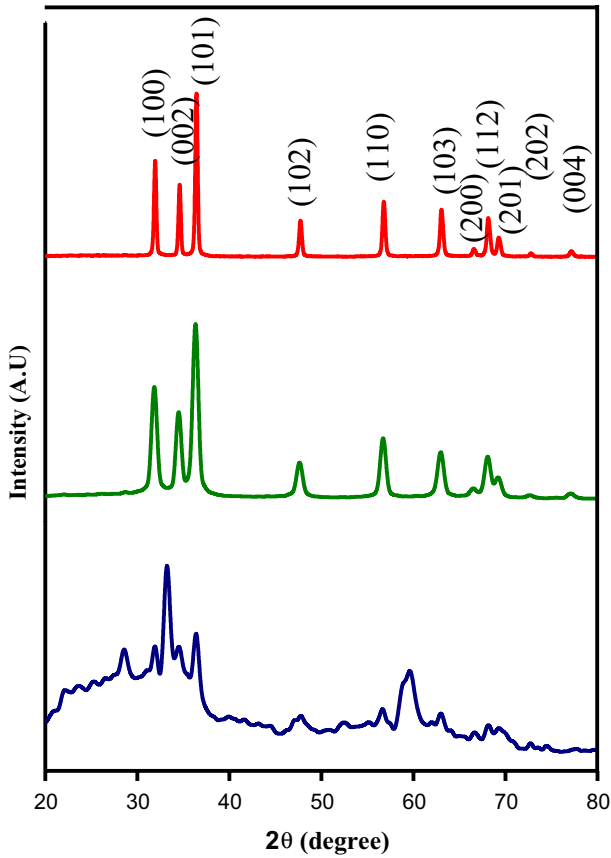


Fig.2 Comparative XRD patterns of **a** ZnO NPs from PE before calcination. **b** ZnO NPs from PE after calcination. **c** ZnO NPs from CM after calcination

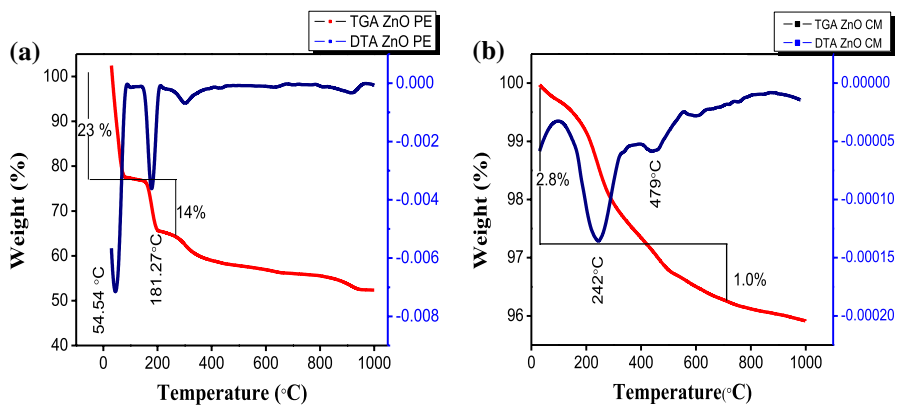
clearly indicates that the extract of neem (*Azadirachta indica*) leaves was effective in controlling the crystallite size of ZnO NPs [6].

TGA and DTA analysis

Herein, TGA and DTA analyses were performed to measure the compositional changes associated with the calcination process, and the results are shown in Fig. 3a, b. Figure 3a shows the TGA and DTA curves for decomposition of ZnO synthesized by plant extract. TGA showed weight loss in two steps at 54 °C and 181 °C, respectively, and corresponding DTA showed two endothermic peaks at these temperatures. It is considered that 23% weight loss at 56 °C is due to the removal of natural products by heating process. Again 14% weight loss at around 181 °C is due to the removal of biomolecules of extract absorbed on surface of

Table 1 2θ values, hkl planes, observed ' d ' values, standard ' d ' values of plant extract and chemical method synthesized ZnO NPs

Sr. no.	2θ values of ZnO-PE NPs	Observed ' d ' values (Å)	2θ values of ZnO-CM NPs	Observed ' d ' values (Å)	Standard ' d ' values (Å)	hkl planes
1	31.87 °	2.8057	31.94°	2.7997	2.8143	100
2	34.46 °	2.6005	34.57°	2.5925	2.6033	002
3	36.31 °	2.4722	36.43°	2.4643	2.4759	101
4	47.63 °	1.9077	47.73°	1.9039	1.9111	102
5	56.67 °	1.6230	56.76°	1.6206	1.6247	110
6	63.12 °	1.4717	63.03°	1.4736	1.4771	103
7	66.50 °	1.4049	66.54°	1.4042	1.4071	200
8	68.06 °	1.3765	68.12°	1.3754	1.3781	112
9	69.20 °	1.3565	69.23°	1.3560	1.3582	201
10	72.58 °	1.3015	72.69°	1.2998	1.3017	004
11	77.09 °	1.2362	77.17°	1.2351	1.2380	202

**Fig. 3** **a** TGA and DTA curves for decomposition of ZnO synthesized by plant extract. **b** TGA and DTA curves for decomposition of ZnO synthesized by chemical method

ZnO NPs [13]. Upon continuation of temperature, the major weight loss was credited toward the loss of natural product and water moisture. In contrast, Fig. 3b shows the TGA and DTA curves for decomposition of ZnO synthesized by chemical method. TGA showed weight loss in two steps at 242 °C and 579 °C, respectively, and corresponding DTA showed two endothermic peaks at these temperatures. It is considered that the weight loss at 242 °C and 479 °C is due to the removal of water by heating process. Synthesis of ZnO from CM is composed of two steps. First is the removal of water and second formation of hexagonal structure by removing water moisture and oxygenated carbon groups [10].

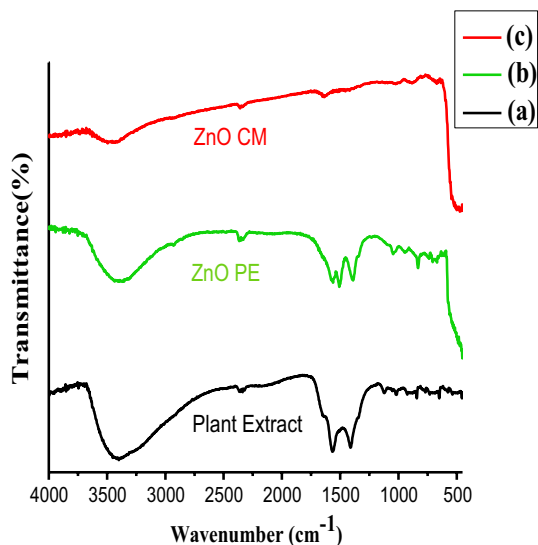
FTIR analysis

For the identification of functional groups, bonding information comparative FTIR spectra were recorded for synthesized ZnO NPs by plant extract and chemical method. The chemical method synthesized ZnO NPs shows a peak at around 3400 cm^{-1} corresponding to the bending and stretching vibration of the $-\text{OH}$ group of the adsorbed water molecules and the peaks at around 450 cm^{-1} indicate metal oxide bond (Fig. 4). On the other hand, the FTIR of ZnO NPs synthesized by PE shows additional peaks at around 1560 cm^{-1} and 1385 cm^{-1} probably due to C–H stretching vibration of CH_2 group and vibration peaks for C=C and C=O bonds, respectively [23]. The peaks at around 1300 cm^{-1} and 842 cm^{-1} are due to the presence of C–N stretch of amine group and C–Br stretch of alkyl halide [10]. The peak at 449 cm^{-1} indicates metal oxide bond [34]. The occurrence of extract-associated bonds in Zn-PE NPs indicates plant extract acts as a capping as well as reducing agent.

FESEM analysis

The size and morphology of the plant extract and chemical method synthesized ZnO NPs were studied using FESEM. Comparative FESEM image under different magnifications, morphology for the plant extract method synthesized ZnO NPs shows mushroom-like mesoporous structure and their diameter range $45\text{--}56\text{ nm}$, while ZnO NPs synthesized by chemical method show hexagonal nanostructure and their diameter range $74\text{--}94\text{ nm}$ observed in Figs. 5c and 6c. In accordance with XRD results, the ZnO NPs synthesized from plant extract were observed in smaller size than the ZnO NPs synthesized from chemical method. This could be attributed to

Fig. 4 FTIR spectra for **a** plant extract (black line); **b** ZnO NPs from PE (green line); **c** ZnO NPs from CM (red line)



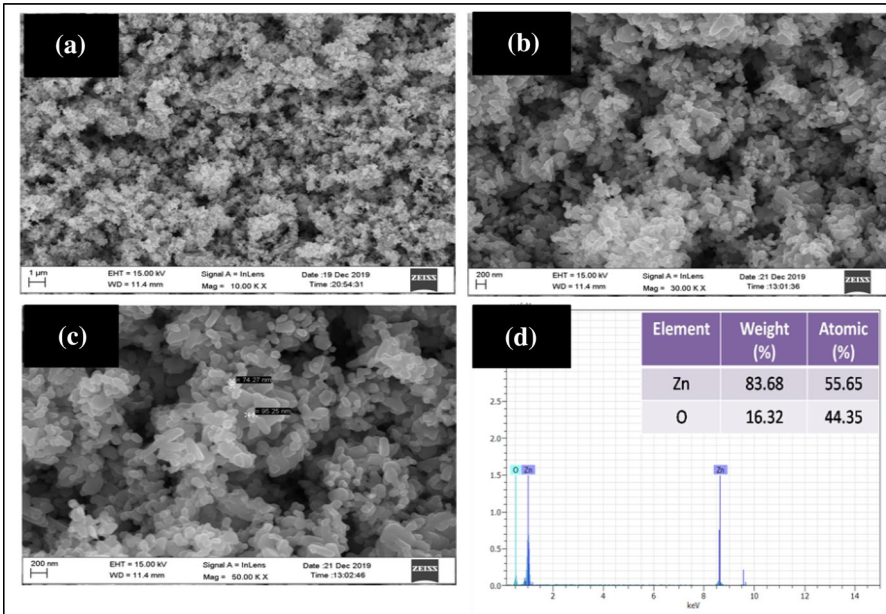


Fig. 5 FESEM images of ZnO NPs synthesized from CM at magnification: **a** 10KX; **b** 30KX; **c** 50KX. **d** EDX analysis of chemical method synthesized ZnO NPs

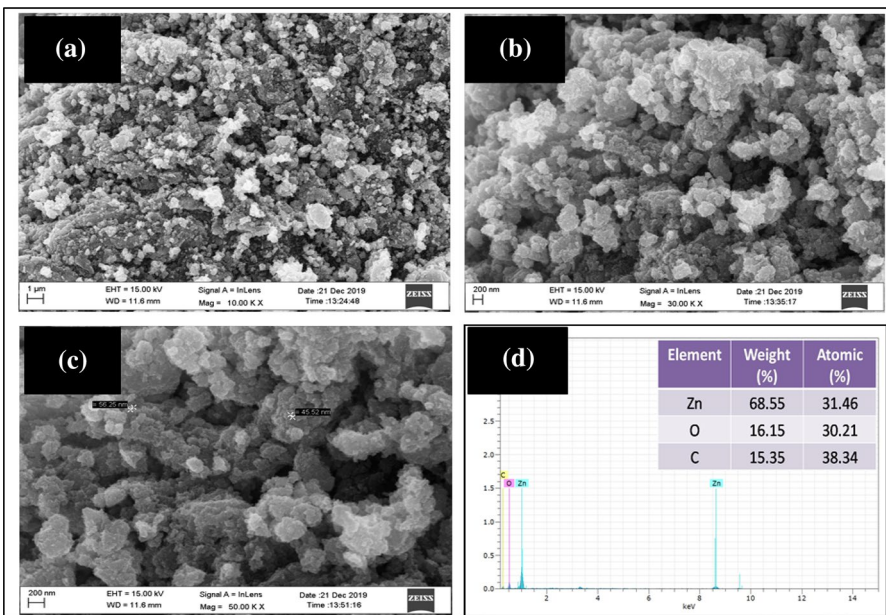


Fig. 6 FESEM images of ZnO NPs synthesized from PE at magnification: **a** 10KX; **b** 30 KX; **c** 50KX. **d** EDX analysis of ZnO-PE NPs

the bioactive compounds of the neem plant extract acting as a stabilizing agent and controlling the growth of the crystallites [10].

EDX analysis

EDX analysis was performed to determine the elemental composition present in the ZnO-CM and ZnO-PE NPs. The EDX spectrum of the ZnO-CM NPs consisted of only two elements, Zn and O (Fig. 5d). On the other hand, the EDX spectrum of the ZnO-PE NPs consisted of three elements, Zn, O and C (Fig. 6d). The presence of C in the peak indicates that organic molecules from the neem plant extract were used as capping agents during the formation of the ZnO NPs [34].

Optical measurement

Optical properties of synthesized nanomaterials were studied by using UV–visible spectrometer in the range of 300–800 nm. The optical absorption spectrum of ZnO NPs (prepared by chemical and plant extract methods) is studied as shown in Fig. 7a. The blueshift is perceived in case of plant extract, which indicates lower particle size of ZnO NPs [35]. The enhanced photoactivity of ZnO-PE was further confirmed via computing the band gap energies (E_g) of both ZnO samples by plotting the graph of $(\alpha h\nu)^2$ versus $(h\nu)$ in Fig. 7b. This provided an estimate on the E_g of ZnO-CM and ZnO-PE which were 3.14 eV and 2.95 eV, respectively, and supported the results.

BET analysis

In order to investigate the effect of the extract on the surface characteristics of ZnO, nitrogen adsorption–desorption trials were recorded and are shown in Fig. 8. A wide distribution of pores and multilayer adsorption on the surface

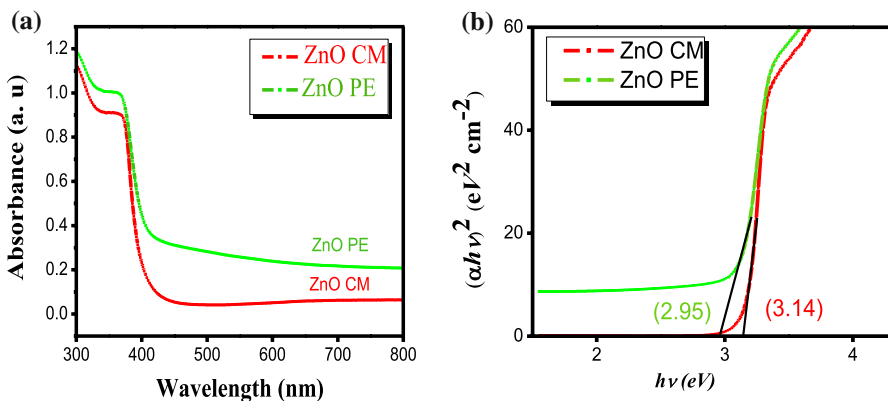


Fig. 7 a Optical absorption spectrum and b $(\alpha h\nu)^2$ versus $(h\nu)$

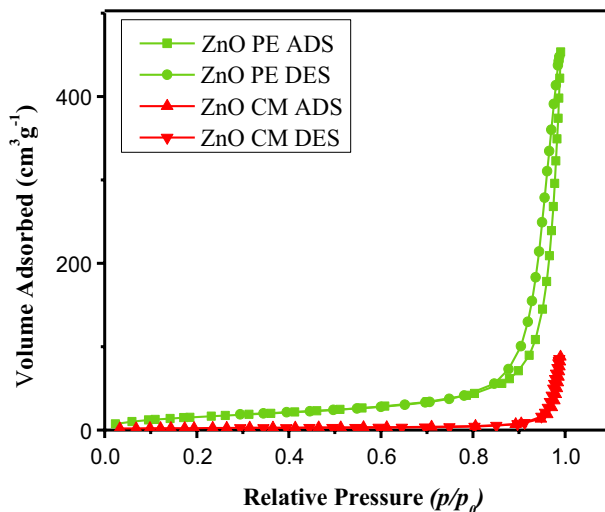


Fig. 8 Isotherms of nitrogen adsorption–desorption of ZnO samples

were obtained for ZnO-CM and ZnO-PE NPs, as proven by the typical type III isotherm. As a result, ZnO-PE possesses remarkably large BET surface area and pore volume compared to ZnO-CM; these BET surface areas are $58.862 \text{ m}^2 \text{ g}^{-1}$ and $8.1624 \text{ m}^2 \text{ g}^{-1}$ and pore volumes are $0.6897 \text{ cm}^3 \text{ g}^{-1}$ and $0.1349 \text{ cm}^3 \text{ g}^{-1}$, respectively (Table 2). These results imply that the adsorption capacity of ZnO-PE will be much higher than that of ZnO-CM [36]. Meanwhile, the average pore size of ZnO-PE (46 nm) is smaller than that of ZnO-CM (66 nm).

Catalytic application of ZnO NPs and hydrotrope

After successful preparation and characterization of the ZnO NPs, we evaluated its effectiveness for the synthesis of BMN and tetraketone. The catalytic efficiency of plant extract synthesized ZnO NPs was checked via synthesizing benzylidenemalonitrile and tetraketone in ZnO NPs/NaPTS catalytic system. With the aim of developing green protocol to be the crucial for rendering the reaction possible in aqueous medium, we carried out long screening test employing 3,4,5-trimethoxy benzaldehyde (1 mmol) and malononitrile (1 mmol) as a model reaction to optimize the parameters such as solvent, time and amount of catalyst.

Table 2 Structural properties of ZnO samples (BET analysis)

Sample	BET surface area ($\text{m}^2 \text{ g}^{-1}$)	Pore volume ($\text{cm}^3 \text{ g}^{-1}$)	Average pore size (nm)
ZnO-CM	8.1624	0.1349	66.097
ZnO-PE	58.862	0.6897	46.867

First, we carried out the reaction in the absence of catalyst and observed that reaction proceeded with trace amount of product after 12 h at room temperature. Then, the reaction was carried out in water at 60 °C and observed that reaction did not proceed efficiently and the product was isolated in 41% yield (Table 3). This negative result highlighted the necessity of catalyst for the present transformation. Among the Lewis acid catalysts BF_3 , TiCl_4 , InCl_3 shows no significant improvement in the yield. After screening Lewis acid, we applied metal oxide in water. Interestingly, we observed that ZnO was most effective for the selected transformation. In comparison, ZnO NPs show an outstanding activity than bulk ZnO in the formation of desired product. Further, we screened the effect of the different solvents. In the presence of acetonitrile and chloroform, poor yields were obtained; on the other hand, in the presence of water, hexagonal and mesoporous ZnO NPs catalyzed model reaction yielded 56% and 65%, respectively. To follow green protocol, we turn our attention toward the water as a solvent for this reaction. Indeed, under aqueous medium reaction was not satisfactory due to less solubility of reactants. Keeping the view of various disadvantages of water, we turned our attention toward the use of hydrotrope as an efficient solvent as well as a phase transfer catalyst. Hydrotropic solution is one of the best alternative solvents for organic transformation. Hydrotrope solubilizes the organic compounds and acts as a catalyst to create hydrophobic environment in water. Among the various hydrotropes, NaPTS is better due to its non-hazardous, eco-friendly nature. Remarkably, the yield was increased up to 70% and 75%, when water/NaPTS was

Table 3 Screening of catalyst, solvents and reaction conditions

Sr. no.	Catalyst	Solvent	Condition °C	Time (hr)	Yield 1d (%) [#]	Yield 2p (%) [#]
1	–	Water	RT	12	–	–
2	–	Water	60	12	41	–
3	–	NaPTS (20%)	RT	2	52	42
4	BF_3	Water	60	6	37	Trace
5	TiCl_4	Water	60	6	41	Trace
6	AlCl_3	Water	60	6	45	31
7	Bulk ZnO	Water	60	6	56	48
8	ZnO NPs	Water	60	3	65	59
9	ZnO NPs	CHCl_3	RT	2	56	46
10	ZnO NPs	Acetonitrile	RT	2	58	45
11	ZnO NPs	Ethanol	RT	1	75	70
12	ZnO NPs	$\text{EtOH}/\text{H}_2\text{O}$ (1:1)	RT	1	61	65
13	ZnO-CM	Water/NaPTS (20%)	RT	20 min	90	92
14	ZnO-PE	Water/NaPTS (20%)	RT	10 min	96	95
15	ZnO-CM	Water/NaPTS (40%)	RT	20 min	89	85
16	ZnO-PE	Water/NaPTS (40%)	RT	10 min	86	88

Reaction conditions: 3,4,5-trimethoxy benzaldehyde (1 mmol), malononitrile (1 mmol) and dimedone (2 mmol)

[#]The yields are related to the isolated products

Table 4 Effect of ZnO loading on the yield of the reaction model^a

Entry	Catalyst (mol%)	Catalyst (mol%)	Time (min)	Yield 1d (%) [#]	TON [§]	TOF [*]
1	Nano-ZnOCM	5 mol%	20	35	28	84
2	Nano-ZnO-PE	5 mol%	10	41	32.8	196.4
3	Nano-ZnO-CM	10 mol%	20	90	36.0	108
4	Nano-ZnO-PE	10 mol%	10	96	38.4	229.9
5	Nano-ZnO-CM	15 mol%	20	72	19.2	57.6
6	Nano-ZnO-PE	15 mol%	10	75	20	119.8

^aReaction conditions: 3,4,5-trimethoxy benzaldehyde (1 mmol), malononitrile (1 mmol) in water/NaPTS (20%) at room temperature

[#]Isolated pure products

[§]TON is the moles of 3,4,5-trimethoxy benzaldehyde converted per mole of catalyst

^{*}TOF is defined as $\text{mol}_{\text{product}} \text{mol}^{-1}_{\text{ZnO}} \text{h}^{-1}$

Table 5 Effect of ZnO loading on the yield of the reaction model^a

Entry	Catalyst (mol%)	Catalyst (mol%)	Time (min)	Yield 2p (%) [#]	TON [§]	TOF [*]
1	Nano-ZnOCM	5 mol%	30	34	27.2	54.4
2	Nano-ZnO-PE	5 mol%	20	39	31.2	93.6
3	Nano-ZnO-CM	10 mol%	30	92	36.8	73.6
4	Nano-ZnO-PE	10 mol%	20	95	38.0	114
5	Nano-ZnO-CM	15 mol%	30	68	18.13	36.3
6	Nano-ZnO-PE	15 mol%	20	71	18.93	56.7

^aReaction conditions: 3,4,5-trimethoxy benzaldehyde (1 mmol) and dimedone (2 mmol) in water/NaPTS (20%) at room temperature

[#]Isolated pure products

[§]TON is the moles of 3,4,5-trimethoxy benzaldehyde converted per mole of catalyst

^{*}TOF is defined as $\text{mol}_{\text{product}} \text{mol}^{-1}_{\text{ZnO}} \text{h}^{-1}$

used as a solvent at room temperature (Table 3). It is noteworthy that the ZnO NPs/NaPTS catalytic system affords the finest result in comparison with other catalytic system. Further, we optimized a model reaction for ZnO NPs/NaPTS catalytic system and obtained the remarkable increase in yield up to 95% in just 10 min. It is concluded that ZnO NPs are the best catalyst in aqueous hydrotropic solution of NaPTS at room temperature for the synthesis of BMN and tetraketone. After selection of reaction medium, the model reaction was optimized for catalyst loading (Tables 4, 5). The use of 5 mol% ZnO NPs diminished the quantity of the yield, whereas the yield of product also decreased when used 15 mol% ZnO NPs. The results are excellent at 10 mol% of ZnO NPs. To optimize the quantity (%) of NaPTS for solvent, the model reaction was carried out with 10%, 20%, 30%, 40% and 50% NaPTS solution. The results are excellent at 20% of NaPTS (Fig. 9). The yield of product remains constant for 30% and above concentration. Next, we carried out comparison in between plant extract and chemically synthesized ZnO

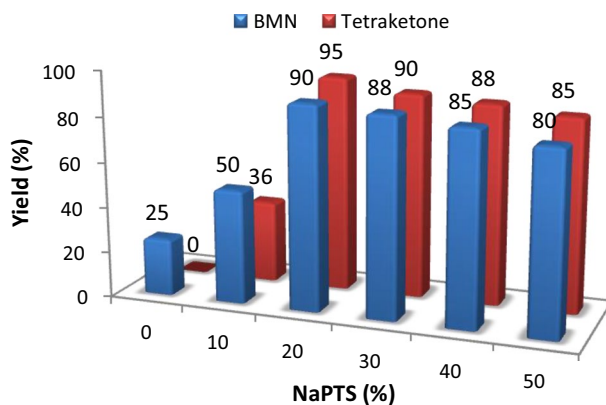
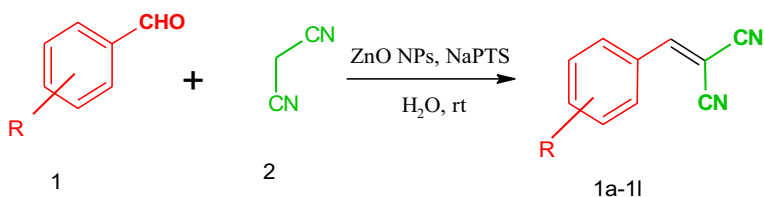


Fig. 9 Effect of amount of NaPTS on the yield of reaction



Scheme 1 Synthesis of benzylidenemalonitrile (BMN)

NPs. Fortunately, result substantiates our hypothesis and the reaction carried out in the presence of plant extract synthesized ZnO NPs with NaPTS in water, not only would be faster but would also result in higher yields as compared to chemical method synthesized ZnO NPs at room temperature. This is probably due to the reason that ZnO NPs prepared from plant extract have mesoporous shape with less crystalline size and high surface area. The Knoevenagel reaction was then performed with various aromatic aldehyde and malonitrile using the optimized amount of catalyst in water (Scheme 1) as shown in Table 6. Next, the efficiency of ZnO-PE for promoting the synthesis of tetraketone derivatives was investigated via the Knoevenagel reaction, followed by Michael addition of an aldehyde with two equivalent of dimedone (Scheme 2) as shown in Table 7.

A plausible mechanistic pathway for the formation of BMN and tetraketone is outlined in Scheme 3. ZnO NPs activate active methylene compound so that deprotonation of the C–H bond occurs and forms intermediate (I) [37]; on the other hand, hydrotrope NaPTS micelles surround aromatic aldehyde through carbonyl oxygen and make carbonyl carbon more electron-deficient carbon, which enhances interaction between reactant and ZnO catalytic system [38].

Tables 8 and 9 show the comparison of the efficiency of ZnO-PE and ZnO-CM NPs with some of the previously introduced procedures to demonstrate its catalytic activity for the synthesis of tetraketone and BMN. It was found that the best

Table 6 Derivatives of benzylidenemalonitrile (BMN)

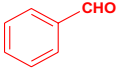
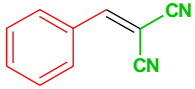
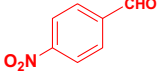
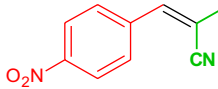
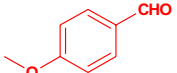
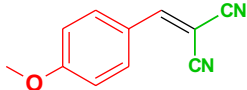
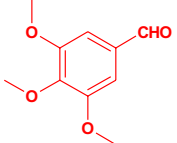
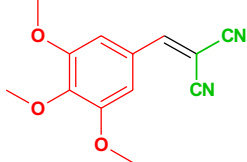
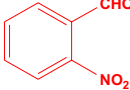
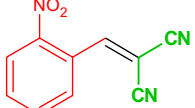
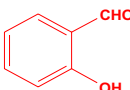
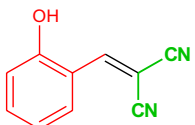
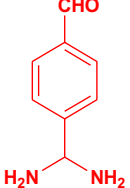
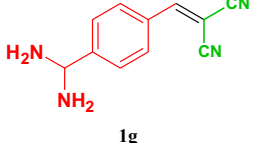
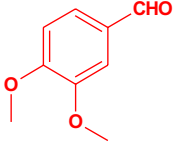
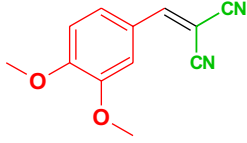
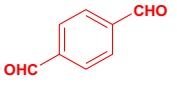
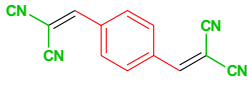
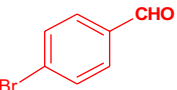
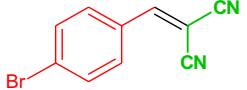
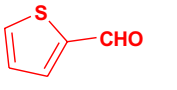
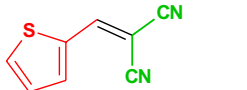
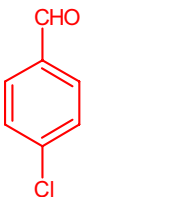
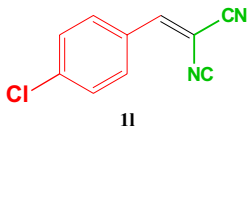
Entry	Aldehyde (1 mmol)	Product	M.P (Obs.)°C	M.P (Theo.) °C	Yield (%)	TOF*
1		 1a	80	85 [14]	90	215.6
2		 1b	160	160 [14]	96	229.9
3		 1c	118	119 [14]	94	225.1
4		 1d	120	122 [39]	96	229.9
5		 1e	140	198 [14]	90	215.6
6		 1f	101	99 [14]	85	203.6
7		 1g	124	125 [40]	90	215.6

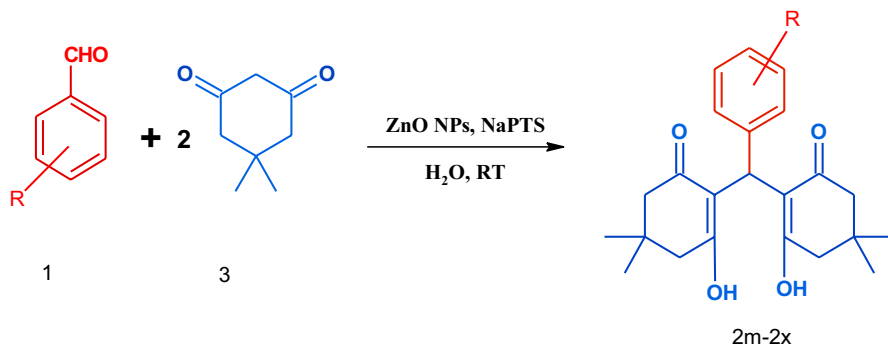
Table 6 (continued)

Entry	Aldehyde (1 mmol)	Product	M.P (Obs.) °C	M.P (Theo.) °C	Yield (%)	TOF*
8		 1h	120	122 [14]	90	215.6
9		 1i	296	296 [14]	94	225.1
10		 1j	154	156 [14]	85	203.6
11		 1k	102	102 [40]	80	191.6
12		 1l	160	162 [14]	95	227.5

Reaction condition: aldehyde (1 mmol), malononitrile (1 mmol), ZnO NPs (10 mol %), NaPTS (20%) distilled water (5 ml)

*TOF is defined as $\text{mol}_{\text{product}} \text{mol}^{-1}_{\text{ZnO}} \text{h}^{-1}$

result could be achieved by using ZnO-PE as indicated by high TOF for BMN 229.9 h^{-1} and for tetraketone 114 h^{-1} . This result is in agreement with our working hypothesis that the most surfaces of these attached ZnO-PE NPs are exposed to the reaction environment. Hence obviously, ZnO-PE NPs show higher catalytic activity in comparison with others in terms of catalyst loading, required reaction time, product yield and avoiding the use of toxic solvents.



Scheme 2 Synthesis of tetraketone

Recyclability

For any chemical process, recovery and recyclability of catalyst are very important. In the present context, recovery of catalyst as well as reaction medium increases the aspect of sustainability. After completion of reaction, ZnO NPs (catalyst) were separated by using centrifugation. It was then dried in a hot air oven to reactivate the catalyst reaction sites. The recyclability chart of the catalytic potential of the ZnO NPs synthesized from plant extract is shown in Fig. 10. An approximately 15% loss of conversion was observed after the fifth cycle of the reaction. The product was separated by adding (5 mL) water in reaction mixture, and the solid product was filtered off. A recovered aqueous layer of hydrotropic medium was washed with ethyl acetate (5 mL) to remove organic compounds. The aqueous layer was concentrated by adding required amount NaPTS or evaporating water under vacuum [50]. The aqueous layer of NaPTS and dried ZnO NPs was reused for the next five reaction cycles. Further, in order to investigate the stability of nano-ZnO synthesized from plant extract during five runs, XRD pattern of the fresh ZnO NPs was compared with the recovered one after the fifth cycle; XRD spectra displayed by the recovered catalyst were found to be almost similar to the fresh one (Fig. 11).

Spectroscopic data

Benzylidenepropanedinitrile (1a)

Buff white crystalline solid, mp 80 °C, IR (KBr, cm⁻¹): 2990, 2210, 1590, 1510, 1220. ¹H NMR (400 MHz, CDCl₃): δ = 7.5 (q, 2H, Ar-H), 7.6 (m, 1H, Ar-H), 7.7 (s, 1H, C=CH), 7.9 (t, 2H, Ar-H) ppm; ¹³C NMR (100 MHz, CDCl₃): δ = 82.84, 112.57, 113.73, 129.65, 130.76, 130.92, 134.67, 160.00 ppm.

Table 7 Different derivatives of tetraketones

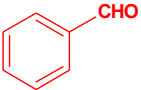
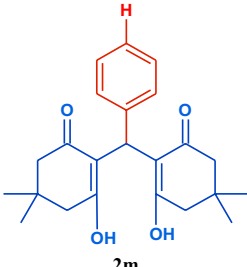
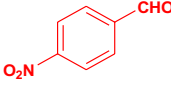
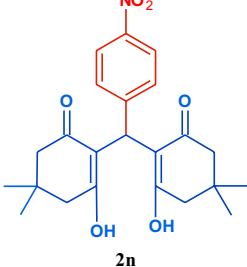
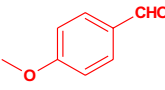
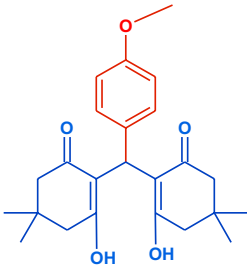
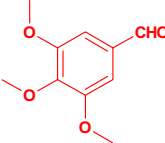
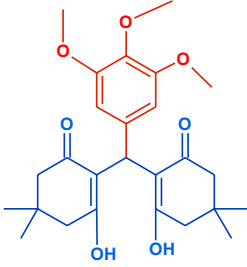
Entry	Aldehyde (1 mmol)	Product	M.P (Obs.) °C	M.P (Theo.) °C	Yield (%)	TOF*
1		 2m	196	195 [23]	95	114.0
2		 2n	192	192 [23]	90	108
3		 2o	144	145 [23]	92	110.4
4		 2p	193	190 [41]	95	114

Table 7 (continued)

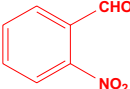
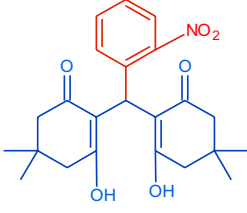
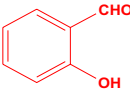
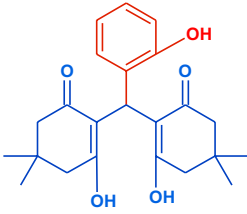
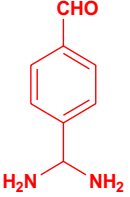
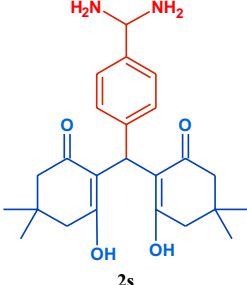
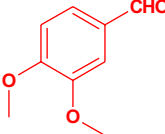
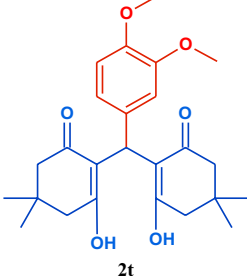
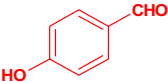
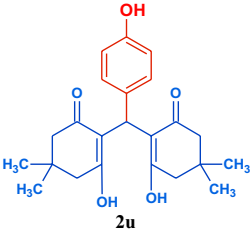
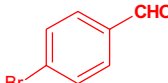
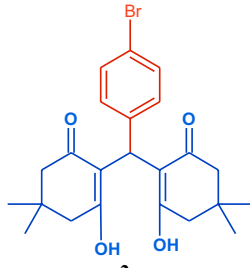
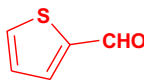
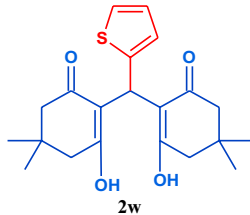
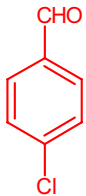
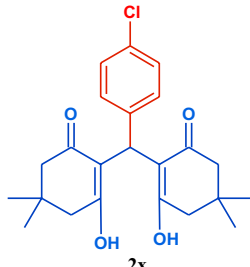
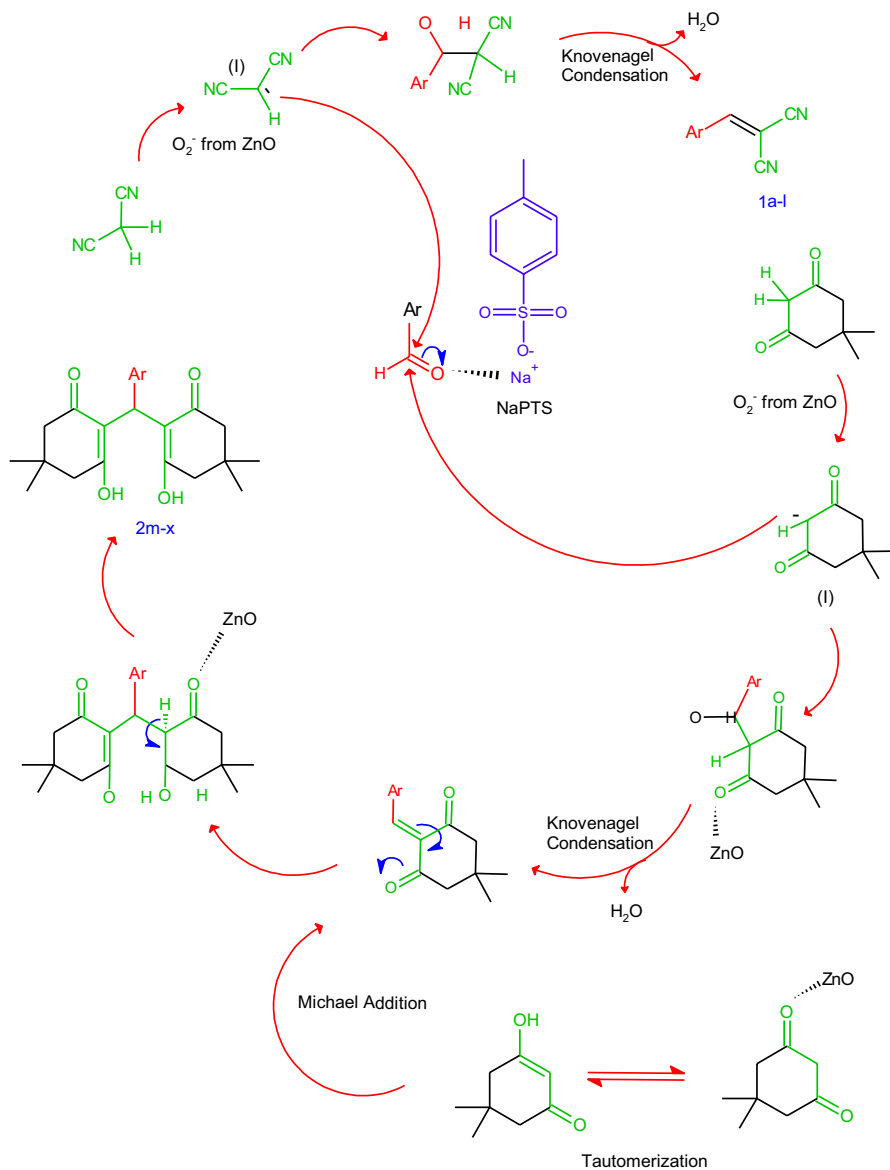
Entry	Aldehyde (1 mmol)	Product	M.P (Obs.) °C	M.P (Theo.) °C	Yield (%)	TOF*
5		 2q	192	190 [23]	90	108
6		 2r	182	180 [41]	85	102
7		 2s	195	195 [41]	90	108
8		 2t	180	183 [41]	91	109.2

Table 7 (continued)

Entry	Aldehyde (1 mmol)	Product	M.P (Obs.) °C	M.P (Theo.) °C	Yield (%)	TOF*
9		 2u	190	188 [23]	40	48
10		 2v	155	155 [23]	85	102
11		 2w	218	216 [23]	90	108
12		 2x	144	140 [23]	93	111.6

Reaction condition: aldehyde (1 mmol), 1,3-cyclohexanedione (2 mmol), ZnO NPs (10 mol %), NaPTS (20%), distilled water (5 ml)

*TOF is defined as $\text{mol}_{\text{product}} \text{mol}^{-1}_{\text{ZnO}} \text{h}^{-1}$



Scheme 3 The plausible mechanism of the studied reaction in the presence of ZnO NPs in aqueous hydrotropic medium

[(4-Nitrophenyl)methylidene]propanedinitrile (**1b**)

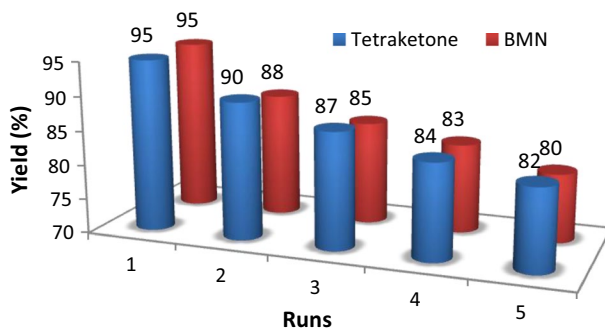
Golden yellow crystalline solid, mp 160 °C, IR (KBr, cm^{-1}): 2950, 2215, 1515, 1350. ^1H NMR (400 MHz, CDCl_3): $\delta=7.5$ (dd, $J=4$ Hz, 2H, Ar-H), 7.7 (s, 1H,

Table 8 Comparative synthesis of recently published works for the BMN versus present work

Catalyst	Solvent	Temp. (°C)	Time (Min)	Yield (%)	References
Go/PdNi NPs	EtOH/H ₂ O (1:1)	RT	8	95	[39]
Taurine	H ₂ O	Reflux	14	86	[14]
Fe ₃ O ₄ –cystamine	EtOH/H ₂ O (1:1)	50	20	93	[40]
GO (1.5 mg/mL)	Solvent-free	RT	80	92	[42]
Ni–Zn–Fe @ SiO ₂	H ₂ O	Reflux	15	97	[43]
Lemon juice	H ₂ O	RT	15	90	[44]
MOF-Pd	DMSO d ₆	RT	5	42	[45]
PMVO 1	Solvent-free	70	45	86	[46]
ZnO NPs PE	H ₂ O (20% NaPTS)	RT	10	95	Present work
ZnO NPs CM	H ₂ O (20% NaPTS)	RT	20	93	Present work

Table 9 Comparative synthesis of the recently published works for the tetraketone versus present work

Catalyst	Solvent	Temp. (°C)	Time (min)	Yield (%)	References
–	H ₂ O	25	240	96	[47]
CoFe ₂ O ₄ NPs	Water/ethanol (1:1)	60	40	89	[48]
Fe ₃ O ₄ @SiO ₂ SO ₃ H	H ₂ O	rt	80	83	[41]
Nano-Fe/NaY zeolite	EtOH	78	70	98	[49]
Ni–Zn–Fe @ SiO ₂	H ₂ O	Reflux	15	90	[43]
GO/ZnO	H ₂ O	100	10	98	[23]
Taurine	H ₂ O	Reflux	20	92	[14]
β -cyclodextrins	H ₂ O	RT	60	93	[25]
ZnO NPs PE	H ₂ O (20% NaPTS)	RT	20	90	Present work
ZnO NPs CM	H ₂ O (20% NaPTS)	RT	30	89	Present work

**Fig. 10** Effect of number of cycles of ZnO NPs on the yield of BMN and tetraketone

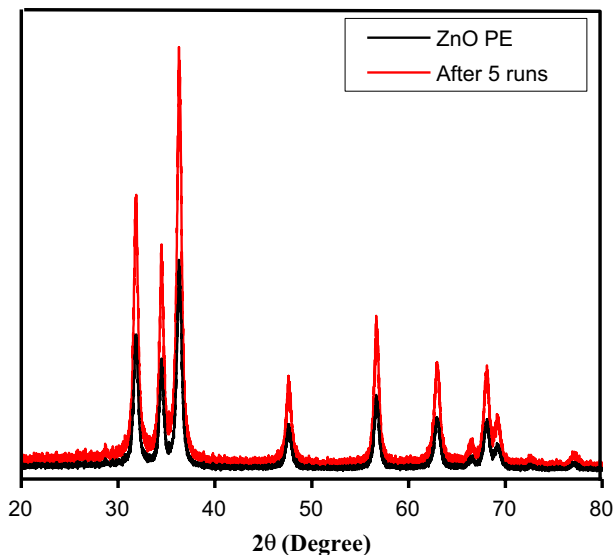


Fig.11 Comparative XRD pattern of fresh ZnO NPs synthesized by plant extract (black line) and after the fifth catalytic cycle (red line)

C=CH), 7.8 (d, 2H, Ar-H) ppm; ^{13}C NMR (100 MHz, CDCl_3): δ = 83.33, 112.34, 113.45, 129.25, 130.09, 131.86, 141.18, 158.30 ppm.

[(4-Methoxyphenyl)methylidene]propanedinitrile(1c)

Light yellow crystalline solid, mp 118 °C, IR (KBr, cm^{-1}): 2210, 1680, 1610, 1520, 1280, 1180. ^1H NMR (400 MHz, CDCl_3): δ = 3.9 (s, 3H, O- CH_3), 7.0 (d, J = 5 Hz, 2H, Ar-H), 7.6 (s, 1H, C=CH), 7.9 (d, J = 5 Hz, 2H, Ar-H) ppm; ^{13}C NMR (100 MHz, CDCl_3): δ = 55.82, 78.50, 113.37, 114.46, 115.14, 124.01, 133.49, 158.92, 164.83 ppm.

[(3,4,5-Trimethoxyphenyl)methylidene]propanedinitrile(1d)

Yellow crystalline solid, mp 120 °C, IR (KBr, cm^{-1}): 2900, 2337, 2220, 1590, 1489, 1119. ^1H NMR (400 MHz, CDCl_3): δ = 3.91 (s, 6H, O- CH_3), 3.99 (s, 3H, O- CH_3), 7.1 (s, 2H, Ar-H), 7.6 (s, 1H, C=CH) ppm; ^{13}C NMR (100 MHz, CDCl_3): δ = 56.35, 61.27, 80.58, 108.26, 113.20, 113.99, 125.94, 143.97, 153.35, 159.42 ppm.

2,2'-((4-Nitrophenyl)methylene)bis(3-hydroxy-5,5-dimethylcyclohex-2-en-1-one) (2n)

White crystalline solid, mp 192 °C, IR (KBr, cm^{-1}): 3450, 2940, 1600, 1510, 1350, 1380. ^1H NMR (400 MHz, CDCl_3): δ = 1.1 (s, 6H, CH_3), 1.2 (s, 6H, CH_3), 2.4 (m, 8H, CH_2), 5.5 (s, 1H, CH), 7.2 (m, 2H, Ar-H), 8.1 (m, 2H, Ar-H), 11.6 (br, 1H,

OH), 11.8 (s, 1H, OH) ppm; ^{13}C NMR (100 MHz, CDCl_3): δ =27.43, 29.57, 31.46, 33.24, 46.38, 46.96, 114.90, 123.54, 127.64, 146.09, 146.51, 189.61, 190.98 ppm.

2,2'-((3,4,5-Trimethoxyphenyl)methylene) bis(3-hydroxy-5,5-dimethylcyclohex-2-en-1-one)(2p)

White crystalline solid, mp 193 °C, IR (KBr, cm^{-1}): 3440, 2950, 1600, 1510, 1380, 1120. ^1H NMR (400 MHz, CDCl_3): δ =1.1(s, 6H, CH_3), 1.2 (s, 6H, CH_3), 2.3 (m, 8H, CH_2), 3.7 (s, 6H, $\text{O}-\text{CH}_3$), 3.8(s, 3H, $\text{O}-\text{CH}_3$), 5.5 (s, 1H, CH), 6.3 (s, 2H, Ar-H), 11.6 (br, 1H, OH), 12.04 (s, 1H, OH) ppm; ^{13}C NMR (100 MHz, CDCl_3): δ =26.78, 30.07, 31.10, 32.76, 46.31, 47.08, 55.85, 60.88, 104.06, 115.57, 133.74, 135.83, 152.82, 189.34, 190.45 ppm.

Conclusion

We successfully synthesized different morphological forms of ZnO NPs. Its characterization results reveal that ZnO NPs synthesized from plant extract of neem grew in smaller size with high surface area and hence exhibit good catalytic performance. Highly efficient two-component and pseudo-three-component reactions of aryl aldehydes and active methylene compound at room temperature in aqueous medium have been developed for the synthesis of benzylidenemalonitrile and tetraketone derivatives. ZnO NPs synthesized from plant extract give product in very short reaction time with high yield as compared to chemical method synthesized ZnO NPs. Changes in the reaction rate are expected due to the synergistic effect of ZnO-PE NPs and NaPTS. This method gives several advantages including chromatography-free separation, reusable catalyst and reusable hydrotropic medium which follow strictly green protocol.

Acknowledgements The authors gratefully acknowledge the financial support from the Department of Science Technology–Science and Engineering Research Board (DST-SERB) and University Grants Commission (UGC) as major research project and Y.C.I.S. Satara (Autonomous) as seed money. The authors are also thankful to the (DST-FIST) Analytical Instrumentation Lab, Jaysingpur College, Jaysingpur, for providing BET and UVDRS analysis. One of the authors S.A. thanks Krishna Mahavidyalaya, Rethare, for the partial support.

Compliance with ethical standards

Conflict of interest The authors declare that they have no conflicts to declare.

References

1. R.A. Sheldon, *Green Chem.* **72**, 67 (2005)
2. F. Mohammadi, M. Yousefi, R. Ghahremanzadeh, *Adv. J. Chem. Sect. A* **2**, 266 (2019)
3. H. R. Madan, S. C. Sharma, Udayabhanu, D. Suresh, Y. S. Vidya, H. Nagabhushana, H. Rajanaik, K. S. Anantharaju, S. C. Prashantha, P. Sadananda Maiya, *Spectrochimica Acta Part A*, 1386 (2015)
4. A. Kumar, D. Saxena, M.K. Gupta, *Green Chem.* **10**, 2699 (2013)

5. P.C. Nagajyothi, T.N. Minh An, T.V.M. Sreekanth, J.I. Lee, D.J. Lee, K.D. Lee, *Mater. Lett.* **108**, 160 (2013)
6. H. Gao, R. Tayebee, M.F. Abdizadeh, E. Mansouri, M. Latifinia, Z. Pourmojahed, *RSC Adv.* **10**, 3005 (2020)
7. A. Maleki, P. Ravaghi, M. Aghaei, *Res. Chem. Intermed.* (2017)
8. S. Kamble, A. Kumbhar, G. Rashinkar, M. Barge, R. Salunkhe, *Ultrasound Sonochem.* **19**, 812 (2012)
9. A. Maleki, *Ultrasound Sonochem.* **28**, 115 (2017)
10. T. Bhuyan, K. Mishra, M. Khanuja, R. Prasad, A. Varma, *Mater. Sci. Semicond. Process.* **32**, 55 (2015)
11. J.S. Rathore, M. Upadhyay, *Res. J. Pharm. Sci.* **2**, 15 (2013)
12. D. Nath, P. Banerjee, *Environ. Toxicol. Pharmacol.* **33**, 997 (2013)
13. A. Bayrami, S. Alioghli, S.R. Pouran, A.H. Yangjeh, A. Khataee, S. Ramesh, *Ultrasound Sonochem.* **55**, 57 (2019)
14. F. Shirini, N. Daneshvar, *RSC Adv.* **6**, 110190 (2016)
15. K.M. Parida, D. Rath, *J. Mol. Catal. A: Chem.* **310**, 93 (2009)
16. B. Karmakar, B. Chowdhury, J. Banerji, *Catal. Commun.* **11**, 601 (2010)
17. U.P.N. Tran, K.K.A. Le, N.T.S. Phan, *ACS Catal.* **1**, 120 (2011)
18. R.A. Agarwal, S. Mukherjee, *Polyhedron* **105**, 228 (2016)
19. A. Karmakar, A. Paul, K.T. Mahmudov, M.F.C. Guedes Da Silva, A.J.L. Pombeiro, *New J. Chem.* **40**, 1535 (2016)
20. A. Taher, D.-J.J. Lee, B.-K.K. Lee, I.-M.M. Lee, *Synlett* **27**, 1433 (2016)
21. A. Zanon, S. Chaemchuen, F. Verpoort, *Catal. Lett.* **147**, 2410 (2017)
22. H. Goksu, E. Gu, H. Goksu, E. Gultekin, *Chem. Select* **2**, 458 (2017)
23. S. Hasanazadeh Banakar, M.G. Dekamin, A. Yaghoubi, *New J. Chem.* **42**, 14246 (2018)
24. D.H. Jung, Y.R. Lee, S.H. Kim, W.S. Lyoo, *Bull. Korean Chem. Soc.* **30**, 1989 (2009)
25. Y. Ren, B. Yang, X. Liao, *RSC Adv.* **6**, 22034 (2016)
26. M. Rastroshan, S. Sayyahi, V. Zare-Shahabadi, R. Badri, *J. Iranian Chem Res.* **5**, 265 (2012)
27. A. Ilangovan, S. Malayappasamy, S. Muralidharan, S. Maruthamuthu, *Chem. Cent. J.* **5**, 81 (2011)
28. N. Azizi, S. Dezfooli, M.M. Hashemi, *C. R. Chim.* **16**, 997 (2013)
29. J. Khurana, K. Vij, *J. Chem. Sci.* **124**, 907 (2012)
30. S. Das, S. Paul, *J. Chem. Inf. Model* **57**, 1461 (2017)
31. S.D. Sharma, P. Gogoy, D. Konwar, *Green Chem.* **9**, 153 (2007)
32. M.R. Parra, F.Z. Haque, *J. Mater. Res. Technol.* **3**(4), 363 (2014)
33. MdR Shakil, A.G. Meguerdichian, H. Tasnim, A. Shirazi-Amin, M.S. Seraji, S. Suib, *Inorg. Chem.* (2019)
34. M.H. Kahsay, A. Tadesse, D. Rama Devi, N. Belachew, K. Basavaiah, *RSC Adv.* **9**, 36967 (2019)
35. B. Shinde, S. Kamble, P. Gaikwad, V. Ghanwat, S. Tanpure, P. Pagare, B. Karale, A. Burungale, *Res. Chem. Intermed.* **44**, 3097 (2018)
36. V.N. Pham, Do-Gun Kim, Seok-Oh Ko, *Science of Total Environment* **631**, 609 (2018)
37. P.P. Ghosh, A.R. Das, *J. Org. Chem.* **12**, 6170 (2013)
38. B. Shinde, S.B. Kamble, D.M. Pore, P. Gosavi, A. Gaikwad, H.S. Jadhav, B. Karale, A.S. Burungale, *Chemistry Select* **3**, 13197 (2018)
39. N. Lolak, E. Kuyuldar, H. Burhan, H. Goksu, S. Akocak, F. Sen, *ACS Omega* **4**, 6848 (2019)
40. R. Maleki, E. Kolvari, M. Salehi, M. Koukabi, *Appl. Organomet. Chem.* **31**, 3795 (2017)
41. F. Nemati, M.M. Heravi, R. Saeedi Rad, *Chin. J. Catal.* **33**, 1825 (2012)
42. S.M. Islam, A.S. Roy, R.C. Dey, S. Paul, *J. Mol. Catal. A Chem.* **394**, 66 (2014)
43. M. Gilanizadeh, B. Zeynizadeha, *New J. Chem.* **42**, 8553 (2018)
44. M.B. Deshmukh, S.S. Patil, S.D. Jadhav, P.B. Pawar, *Synth. Commun.* **42**, 1177 (2012)
45. C.I. Ezugwu, B. Mousavi, M.A. Asraf, Z. Luo, F. Verpoort, *J. Catal.* **344**, 445 (2016)
46. B. Viswanadham, P. Jhansi, K.V.R.R. Chary, H.B. Friedrich, S. Singh, *Catal. Lett.* **146**, 364 (2016)
47. Yu Jian-Jun, L.-M. Wang, J.-Q. Liu, F.-L. Guo, Y. Liu, Ning Jiao, *Green Chem.* **12**, 216 (2010)
48. J.K. Rajput, G. Kaur, *Catal. Sci. Technol.* **4**, 142 (2014)
49. M. Tajbakhsh, M. Heidary, R. Hosseinzadeh, *Res. Chem. Intermed.* **42**, 1425 (2016)
50. A. Kumbhar, S. Kamble, M. Barge, G. Rashinkar, R. Salunkhe, *Tetrahedron Lett.* **53**, 2756 (2012)